

Short Note

2-*{(E)-2-[(3E)-2-Chloro-3-*{(2E)-2-[1,1-dimethyl-3-(3-phenylpropyl)-1,3-dihydro-2H-benzo[e]indol-2-ylidene]-ethylidene}*cyclohex-1-en-1-yl]ethenyl}*-1,1-dimethyl-3-(3-phenylpropyl)-1*H*-benzo[e]indolium Iodide

Eric A. Owens^{1,2,3}, Joseph G. Tawney¹ and Maged M. Henary^{1,2,3,*}

¹ Department of Chemistry, Georgia State University, Atlanta, GA 30303, USA

² Center for Diagnostics and Therapeutics, Georgia State University, Atlanta, GA 30303, USA

³ Center for Biotechnology and Drug Design, Georgia State University, Atlanta, GA 30303, USA

* Author to whom correspondence should be addressed; E-Mail: mhenary1@gsu.edu.

Received: 20 December 2013 / Accepted: 22 January 2014 / Published: 30 January 2014

Abstract: In four synthetic steps we successfully prepared a red-shifted heptamethine cyanine dye ($\lambda_{\max} = 825$ nm in methanol) that could be very useful for biochemists and bioanalytical chemists for probing lipophilic environments, including the hydrophobic pockets of enzymes. The heptamethine dye structure was characterized by various spectroscopic techniques including ¹H-NMR, ¹³C-NMR and high-resolution accurate mass spectroscopy (HRMS). We have also shown the hydrophobicity spectrally by varying methanol/water ratios and observing corresponding absorbance and fluorescence spectral changes.

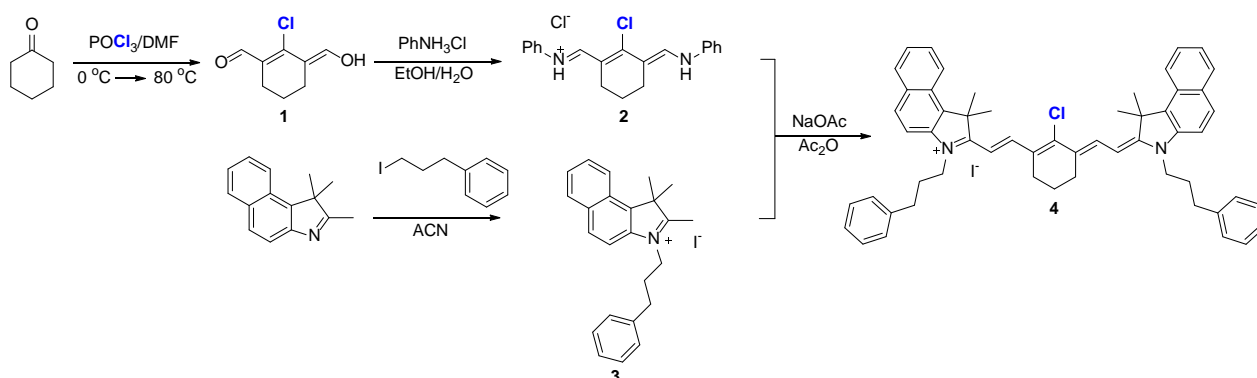
Keywords: Hydrophobicity; carbocyanine; near-infrared; fluorescence; absorption; Vilsmeier-Haack reagent

Introduction

Cyanine dyes are an interesting class of fluorescent compounds that are defined by two terminal heterocyclic nitrogen containing rings that have a delocalized monocation across a polymethine bridge, as compound **4** shown in Scheme 1 [1–5]. The synthetic preparation of these chromophores allows for diverse modifications at various locations to finely tune the binding properties to biomolecules or to modify for achieving very specific wavelengths [6,7]. The high molar extinction coefficient and quantum yield of these compounds have been extensively utilized in various

applications [8]. Specifically, bioanalytical chemists have successfully employed these compounds as non-covalent labels or nucleic acid fluorescent tags [9–11]. We have capitalized on optimum optical properties tailored using the chemical structure by designing a NIR-absorbing and fluorescing heptamethine cyanine dye that reports on the hydrophobicity of its environment. It has been reported throughout the literature that hydrophobic cyanines form non-fluorescent blue-shifted dimers (H-aggregates) after being placed in highly polar environments (water, PBS/FBS buffers, *etc.*) [9–14]. The addition of a biomolecule with hydrophobic pockets will break up the non-fluorescent dimer and form the red-shifted and highly fluorescent monomeric peak; the corresponding optical change allows for the calculation of binding constants using the change in absorption and fluorescence measurements [14]. This can be extremely useful for non-covalently labeling a biomolecule to be studied using any number of analytical techniques, for instance competitive displacement by a newly synthesized drug.

Scheme 1. The synthetic preparation of heptamethine cyanine dye **4**.



Synthesis

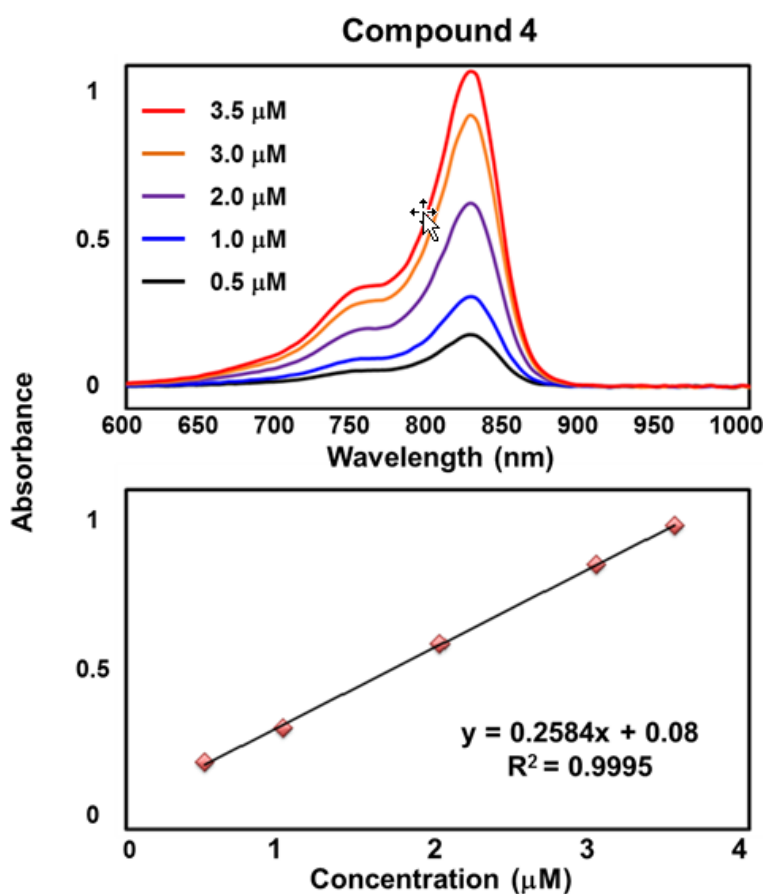
Cyclohexanone was subjected to Vilsmeier formylation to afford bisaldehyde compound **1**, which was then transformed into the Vilsmeier–Haack reagent **2** via the addition of anilinium chloride in a mixture of ethanol and water. In parallel, salt **3** was formed by the S_N2 reaction of 1,1,2-trimethyl-1H-benz[e]indole with 1-iodo-3-phenylpropane in refluxing acetonitrile. Compounds **2** and **3** were allowed to react in a mixture of sodium acetate and acetic anhydride to form a bright green solution containing compound **4**. After isolation, via column chromatography, we successfully prepared, purified, and characterized heptamethine cyanine dye **4** in good yield. We have conveniently incorporated a *meso*-chlorine atom which can be replaced via a well-established $S_{NR}1$ mechanistic pathway where the *meso*-chlorine atom of heptamethine dye is substituted with various nucleofugal functionalities leading to diversely functionalized NIR compounds.

Analytical Determinations

With this lipophilic chromophore **4** in hand, we proceeded to examine the optical profile in methanol, including the molar absorptivity and fluorescence. As shown in Figure 1, the absorbance spectra were recorded at various concentrations (0.5 μ M, 1.0 μ M, 2.0 μ M, 3.0 μ M, 3.5 μ M), and the absorbance values were plotted against concentration. A remarkable signature of cyanine dyes is the elevated extinction coefficient; compound **4** displayed a similar trend with the molar absorptivity being

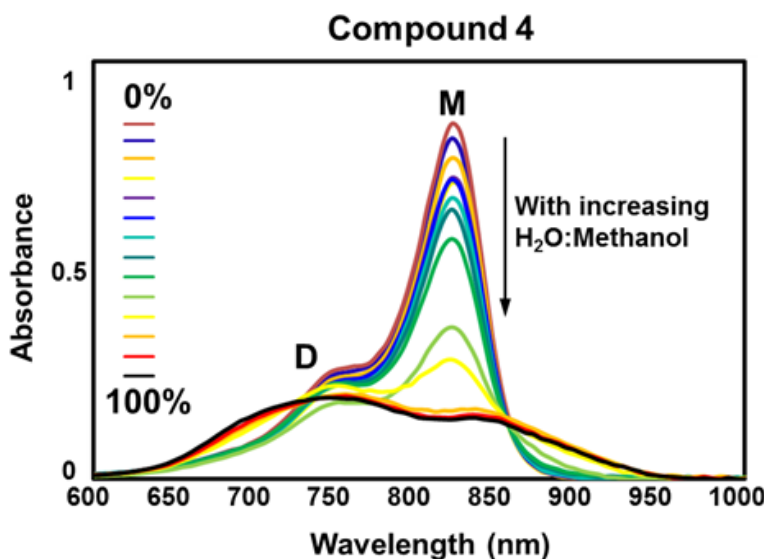
$258,400 \text{ M}^{-1}\text{cm}^{-1}$, which was confirmed in triplicate with excellent linear correlation ($R^2 = 0.9995$). It should be noted that alternate cyanine chromophores are blue shifted compared to our compound **4**. We note a 20–30 nm red-shift when the benz[*e*]indolenine heterocyclic structure is used in the design of the chromophore, which places this particular compound well within the desired therapeutic window of clarity associated with the NIR region [12,13].

Figure 1. (top) The absorbance spectra of compound **4** in methanol at different concentrations (0.5 μM , 1.0 μM , 2.0 μM , 3.0 μM , 3.5 μM). (bottom) The absorbance increase was linear with respect to concentration and follows the Beer-Lambert law with the extinction coefficient being calculated from the linear regression as $\epsilon = 258,400 \text{ M}^{-1}\text{cm}^{-1}$.



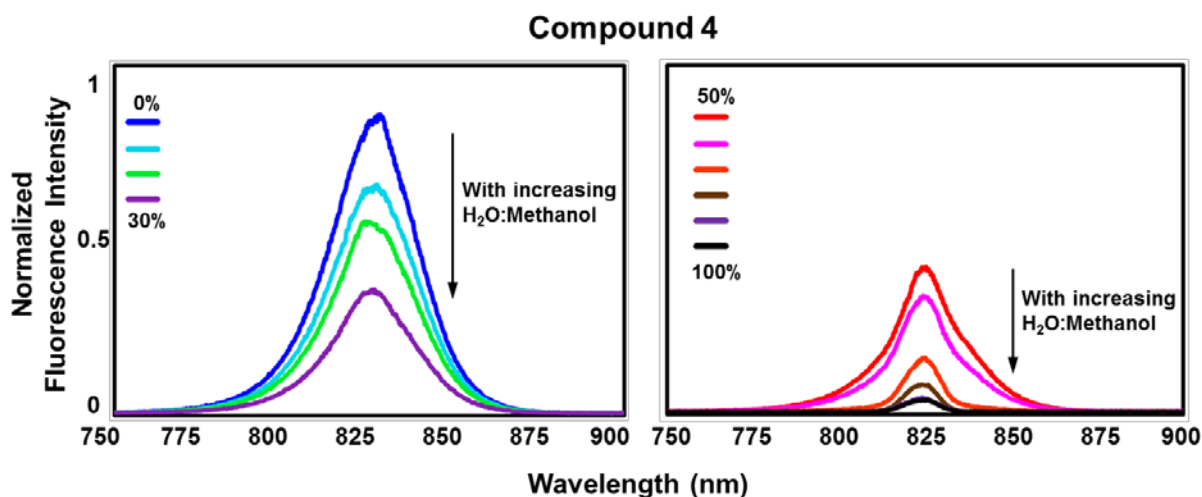
We then wanted to confirm the suspected dimerization phenomenon of highly hydrophobic cyanines. To do this, we gradually increased the polarity of the solvent which was expected to cause dimerization due to hydrophobicity. This phenomenon is characterized by a hypsochromic wavelength shift with a hypochromic absorbance intensity change corresponding to a reduction in the monomer band. In Figure 2, we present the spectra obtained from our hydrophobicity study. The monomer band is labeled **M** (Figure 2) and the dimer band is labeled **D**. The ratio of the two peaks changes drastically with the **D** band showing a higher prevalence (over the monomer band) with increasing water character. The isosbestic point at 855 nm suggests the presence of two species, which, in this case, represents the monomeric and dimeric forms as shown before by our group [14].

Figure 2. The NIR-spectra (600–1000 nm) of compound **4** (2.35 μM) in increasing percentages of water in methanol (0, 10, 20, 30, 40, 45, 50, 55, 60, 65, 70, 80, 90 and 100%) showing a high degree of dimerization and formation of H-aggregates.



We have also observed that H-aggregates tend to show lower fluorescence due to self-quenching through Förster resonance energy transfer [14]. We see this phenomenon occurring upon dimerization in Figure 3. As the water character increases in the dye-solution, the fluorescence decreases corresponding to non-fluorescent aggregation of the compound. At a 1:1 ratio of water to methanol we observe a blue-wavelength shift of 2.6 nm and the fluorescence intensity values continued to decrease.

Figure 3. The NIR fluorescence spectra (750–900 nm) upon excitation at 820 nm of compound **4** (0.1 μM) in increasing percentages of water in methanol (0, 10, 20, 30, 50, 60, 70, 80, 90 and 100%) showing a high degree of dimerization and formation of non-fluorescent H-aggregates.



Experimental

Synthesis

The chemical reagents used in the synthesis of these compounds presented in Scheme 1 were obtained from Acros Organics (Geel, Belgium), Alfa Aesar (Ward Hill, MA, USA) and Matrix Scientific (Columbia, SC, USA). The reactions were followed using silica gel 60 F254 thin layer chromatography plates (Merck EMD Millipore, Darmstadt, Germany) with 5% methanol in dichloromethane (DCM) as the mobile phase. Open column chromatography was utilized for the purification the final using 60-200 μm , 60A classic column silica gel (Dynamic Adsorbents, Norcross, GA, USA). The ^1H -NMR and ^{13}C -NMR spectra were obtained using high quality Kontes NMR tubes (Kimble Chase, Vineland, NJ, USA) rated to 500 MHz and were recorded on a 400 MHz Bruker Avance spectrometer (Bruker Corporation, Billerica, MA, USA) using $\text{DMSO-}d_6$ containing tetramethylsilane (TMS) as an internal calibration standard. High-resolution accurate mass spectra (HRMS) were obtained either at the Georgia State University Mass Spectrometry Facility using a Waters Q-TOF micro (ESI-Q-TOF) mass spectrometer or utilizing a Waters Micromass LCT TOF ES+ Premier Mass Spectrometer (Waters Corporation, Milford, MA, USA). The synthetic procedures for the preparation of **1**, **2**, and **3** have been previously reported by our lab [15,16].

Synthesis of 2-((*E*)-2-((*E*)-2-chloro-3-((*E*)-2-(1,1-dimethyl-3-(3-phenylpropyl)-1,3-dihydro-2H-benzo[*e*]indol-2-ylidene)ethylidene)cyclohex-1-en-1-yl)vinyl)-1,1-dimethyl-3-(3-phenylpropyl)-1H-benzo[*e*]indol-3-ium iodide (**4**): A clean and oven dried 25-mL round bottom flask was cooled under nitrogen atmosphere. Salt **3** (1.2 g, 2.64 mmol) was added with acetic anhydride (10 mL) under heavy stirring. Sodium acetate (216 mg, 2.64 mmol) was then added to deprotonate the acidic alpha-proton of salt **3** and the reaction mixture was heated to 60 °C. After the addition of sodium acetate the salt **3** dissolved in the acetic anhydride. After dissolution, Vilsmeier-Haack reagent **2** (473 mg, 1.32 mmol) was added to the stirring solution. The mixture turned red immediately after the addition of reagent **2**. The mixture was allowed to react at 60 °C for 4 h until the starting materials were consumed as noted by TLC eluting in 2% methanol in DCM and UV-Vis-NIR absorption spectroscopy. Compound **4** was obtained in 72% yield as deep blue-green metallic crystals. MP: 134–136 °C, ^1H -NMR (400 MHz, $\text{DMSO-}d_6$) δ 1.904 (bs, 2H), 1.977 (s, 12H), 2.183 (t, $J = 6.8$ Hz, 4H), 2.495 (bs, 4H), 2.853 (t, $J = 6.8$ Hz, 4H), 4.266 (t, $J = 6.8$ Hz, 4H), 6.042 (d, $J = 14.4$ Hz, 2H), 7.380-7.261 (m, 10H), 7.515 (t, $J = 8.0$ Hz, 2H), 7.601 (d, $J = 8.8$ Hz, 2H), 7.662 (t, $J = 8.0$ Hz, 2H), 8.036 (t, $J = 8.4$ Hz, 4H), 8.274 (d, $J = 8.4$ Hz, 2H), 8.430 (d, $J = 14.4$ Hz, 2H). ^{13}C -NMR (100 MHz, $\text{DMSO-}d_6$) 20.88, 26.44, 27.59, 29.14, 32.57, 44.20, 51.22, 101.47, 112.06, 122.71, 125.48, 126.54, 126.81, 128.01, 128.24, 128.80, 128.92, 130.38, 130.94, 132.06, 134.20, 140.14, 141.29, 142.51, 148.04, 173.95. High-resolution accurate mass spectrum $[\text{M}]^+$ calculated for $[\text{C}_{56}\text{H}_{56}\text{N}_2\text{Cl}]^+$ 791.4127 found 791.4140.

Analytical Instrumentation

Absorbance spectra were measured using a Varian Cary 50 Spectrophotometer (Agilent Technologies, Santa Clara, CA, USA) interfaced to a PC, with a spectral bandwidth of 2 nm. Fluorescence spectra for the heptamethine cyanine dye was obtained using a Shimadzu RF-1501

Spectrofluorophotometer (Shimadzu Scientific Instruments, Columbia, MD, USA) interfaced to a PC, with spectral bandwidths for both excitation and emission set to 10 nm and the sensitivity set to “high”. Disposable absorbance and fluorescence cuvettes (Sigma Aldrich, St. Louis, MO, USA) were used with a pathlength of 1.00 cm. All calculations were performed on Microsoft Excel 2010, (Microsoft Corporation, Redmond, WA, USA).

Preparation of Stock Solutions

Compound **4** was weighed on a 5-digit analytical balance stabilized on a marble table directly into an amber glass vial (Fischer Scientific, Pittsburgh, PA, USA). The solid was diluted into dimethyl sulfoxide (Analytical Grade, 99.9%, Fischer Scientific) to a 1 mM concentration. The vial was capped and vortexed for 30 s then sonicated for 20 min to ensure appropriate dissolution into the solvent.

Determination of Molar Absorptivity

Aliquots of the 1 mM stock solution of compound **4** were taken and diluted to various concentrations (0.5 μ M, 1.0 μ M, 2.0 μ M, 3.0 μ M and 3.5 μ M) in methanol ensuring that the most concentrated sample exhibited absorbance less than 1. The absorbance values at the wavelength of maximum absorption (825 nm in methanol) were determined using a Varian Cary-50 spectrophotometer equipped with an extended wavelength detector and were plotted against concentration using Microsoft Excel and the linear correlation and regression were determined. The results obtained from the data were found to have a linear correlation.

Absorbance Hydrophobicity Studies

Test tubes were filled with 5 mL of methanol and water at different percentages (0, 10, 20, 30, 40, 45, 50, 55, 60, 65, 70, 80, 90 and 100% water). A baseline was performed for each sample at the corresponding water:methanol ratio in 1 cm disposable polystyrene cuvettes. After the baseline was recorded, 10 μ L of the 1 mM stock solution was diluted into the cuvette, forming a 2.35 μ M solution. The spectra of the prepared solutions were then plotted as absorbance *versus* wavelength.

Fluorescence Hydrophobicity Studies

Test tubes were filled with 5 mL of methanol and water at different percentages (0, 10, 20, 30, 40, 50, 60, 70, 80, 90 and 100% water). All fluorescence measurements were performed for compound **4** (at a 0.1 μ M concentration, ensuring $\lambda_{\text{max abs}} < 1$) at the appropriate water-methanol ratio in 1 cm disposable polystyrene cuvettes. After the baseline was recorded, the stock solution was diluted into a test tube, forming a 0.1 μ M solution, which was then transferred into a fluorescence cuvette. The spectra of the prepared solutions were then plotted as fluorescence intensity *versus* wavelength.

Acknowledgments

The authors would like to thank the Center for Diagnostics and Therapeutics (CDT) at Georgia State University for their support. EAO was supported through a CDT fellowship at GSU. The work

was funded by internal research support including a Molecular Basis of Disease (MBD-GSU) grant to MH at GSU.

Conflicts of Interest

The authors declare no conflict of interest

References and Notes

1. Ashitate, Y.; Kim, S.H.; Tanaka, E.; Henary, M.; Choi, H.S.; Frangioni, J.V.; Flaumenhaft, R. Two-wavelength near-infrared fluorescence for the quantitation of drug antiplatelet effects in large animal model systems. *J. Vasc. Surg.* **2012**, *56*, 171–180.
2. Chapman, G.; Henary, M.; Patonay, G. The effect of varying short-chain alkyl substitution on the molar absorptivity and quantum yield of cyanine dyes. *Anal. Chem. Insights* **2011**, *6*, 29–36.
3. Escobedo, J.O.; Rusin, O.; Lim, S.; Strongin, R.M. NIR dyes for bioimaging applications. *Curr. Opin. Chem. Biol.* **2010**, *14*, 64–70.
4. Patonay, G.; Salon, J.; Sowell, J.; Strekowski, L. Noncovalent labeling of biomolecules with red and near-infrared dyes. *Molecules* **2004**, *9*, 40–49.
5. Samanta, A.; Vendrell, M.; Das, R.; Chang, Y.-T. Development of photostable near-infrared cyanine dyes. *Chem. Commun.* **2010**, *46*, 7406–7408.
6. Yang, X.; Shi, C.; Tong, R.; Qian, W.; Zhau, H.E.; Wang, R.; Zhu, G.; Cheng, J.; Yang, V.W.; Cheng, T.; *et al.* Near IR heptamethine cyanine dye-mediated cancer imaging. *Clin. Cancer Res.* **2010**, *16*, 2833–2844.
7. Winstead, A.; Williams, R.; Zhang, Y.; McLean, C.; Oyaghire, S. Microwave synthesis of cyanine dyes. *J. Microwave Power Electromagn. Energy* **2010**, *44*, 207–221.
8. Gu, J.; Anumala, U.R.; Heyny-von Haussen, R.; Holzer, J.; Goetschy-Meyer, V.; Mall, G.; Hilger, I.; Czech, C.; Schmidt, B. Design, synthesis and biological evaluation of trimethine cyanine dyes as fluorescent probes for the detection of tau fibrils in Alzheimer's disease brain and olfactory epithelium. *ChemMedChem* **2013**, *8*, 891–897.
9. Deligeorgiev, T.G.; Vasilev, A.; Drexhage, K.H. Synthesis of novel cyanine dyes containing carbamoyl ethyl component - Noncovalent labels for nucleic acids detection. *Dyes Pigm.* **2007**, *74*, 320–328.
10. Deligeorgiev, T.G.; Zaneva, D.A.; Kim, S.H.; Sabnis, R.W. Preparation of monomethine cyanine dyes for nucleic acid detection. *Dyes Pigm.* **1998**, *37*, 205–211.
11. Zhou, M.; Zhang, X.; Bai, M.; Shen, D.; Xu, B.; Kao, J.; Xia, G.; Achilefu, S. Click reaction-mediated functionalization of near-infrared pyrrolopyrrole cyanine dyes for biological imaging applications. *RSC Adv.* **2013**, *3*, 6756–6758.
12. Owens, E.A.; Hyun, H.; Kim, S.H.; Lee, J.H.; Park, G.; Ashitate, Y.; Choi, J.; Hong, G.H.; Alyabyev, S.; Lee, S.J.; *et al.* Highly charged cyanine fluorophores for trafficking scaffold degradation. *Biomed. Mater.* **2013**, *8*, 014109.
13. Mapp, C.T.; Owens, E.A.; Henary, M.; Grant, K.B. Oxidative cleavage of DNA by pentamethine carbocyanine dyes irradiated with long-wavelength visible light. *Bioorg. Med. Chem. Lett.* **2013**, in press.

14. Beckford, G.; Owens, E.; Henary, M.; Patonay, G. The solvatochromic effects of side chain substitution on the binding interaction of novel tricarbocyanine dyes with human serum albumin. *Talanta* **2012**, *92*, 45–52.
15. Nanjunda, R.; Owens, E.A.; Mickelson, L.; Alyabyev, S.; Kilpatrick, N.; Wang, S.; Henary, M.; Wilson, W.D. Halogenated pentamethine cyanine dyes exhibiting high fidelity for G-quadruplex DNA. *Bioorg. Med. Chem.* **2012**, *20*, 7002–7011.
16. Sinha, S.H.; Owens, E.A.; Feng, Y.; Yang, Y.; Xie, Y.; Tu, Y.; Henary, M.; Zheng, Y.G. Synthesis and evaluation of carbocyanine dyes as PRMT inhibitors and imaging agents. *Eur. J. Med. Chem.* **2012**, *54*, 647–659.

© 2014 by the authors; licensee MDPI, Basel, Switzerland. This article is an open access article distributed under the terms and conditions of the Creative Commons Attribution license (<http://creativecommons.org/licenses/by/3.0/>).